

SCIENTIFIC REPORTS



OPEN

Symmetry Breaking of Counter-Propagating Light in a Nonlinear Resonator

Leonardo Del Bino*, Jonathan M. Silver*, Sarah L. Stebbings & Pascal Del'Haye

Received: 12 January 2017
Accepted: 18 January 2017
Published: 21 February 2017

Spontaneous symmetry breaking is a concept of fundamental importance in many areas of physics, underpinning such diverse phenomena as ferromagnetism, superconductivity, superfluidity and the Higgs mechanism. Here we demonstrate nonreciprocity and spontaneous symmetry breaking between counter-propagating light in dielectric microresonators. The symmetry breaking corresponds to a resonance frequency splitting that allows only one of two counter-propagating (but otherwise identical) states of light to circulate in the resonator. Equivalently, this effect can be seen as the collapse of standing waves and transition to travelling waves within the resonator. We present theoretical calculations to show that the symmetry breaking is induced by Kerr-nonlinearity-mediated interaction between the counter-propagating light. Our findings pave the way for a variety of applications including optically controllable circulators and isolators, all-optical switching, nonlinear-enhanced rotation sensing, optical flip-flops for photonic memories as well as exceptionally sensitive power and refractive index sensors.

Bi-directional propagation of light is an important prerequisite for many types of optical elements including interferometers and resonators. At the same time, nonlinear optical effects have driven many photonic developments in the past decades. Interaction between counterpropagating light has been observed for example in nonlinear loop mirrors^{1,2} and through gain competition in ring lasers^{3–5}. In this work we demonstrate direct Kerr-nonlinearity-mediated light-with-light interaction between counterpropagating modes in a passive ultra-high-Q microresonator. This leads to a spontaneous symmetry breaking between the resonator's clockwise and counterclockwise eigenmodes. In our experiments, a whispering gallery resonator provides the power enhancement to achieve the required light intensities. Such an effect has been theoretically predicted in the 1980s by Kaplan and Meystre in the context of nonlinear enhanced Sagnac interferometry for rotation sensing⁶. Theoretical calculations show that the nonlinear interaction could enable significantly enhanced rotation sensors^{7,8} that are limited only by the relative power stability between the counter-propagating light. In addition the symmetry breaking could be used for precise optical power and refractive index sensing⁹. Equally important, the interaction between counter-propagating waves leads to controllable non-reciprocal propagation of light. In particular, integrated photonic circuits require new ways of achieving non-reciprocal light propagation that do not rely on magneto-optical effects¹⁰. This has been demonstrated using metallic-silicon waveguides¹¹, asymmetric backscattering in microresonators¹², coupled PT-symmetric resonator systems^{13,14}, in asymmetrically coupled systems of microrings¹⁵, and a variety of other devices^{16–19}. Our results rely on direct interaction between counterpropagating light in a Kerr resonator and enable the development of novel types of integrated optical elements including optically controllable diodes, circulators and all-optical flip-flops^{20–23}. In our measurements we show a detailed analysis of the symmetry breaking, which manifests itself as a resonance splitting between the clockwise and counterclockwise microresonator modes. In addition, we perform a threshold power analysis of the nonlinear interaction between counter-propagating light and demonstrate all-optical switching between clockwise and counterclockwise circulating light. Our experimental findings are in excellent agreement with theoretical calculations of Kerr-nonlinearity-induced symmetry breaking and non-reciprocal propagation of light.

The nonlinear interaction between counter-propagating light in a nonlinear Kerr medium is illustrated in Fig. 1a. Crucially, two counter-propagating light waves with equal wavelength outside of a nonlinear Kerr

National Physical Laboratory (NPL), Teddington, TW11 0LW, United Kingdom. *These authors contributed equally to this work. Correspondence and requests for materials should be addressed to P.D.H. (email: pascal.delhaye@npl.co.uk)

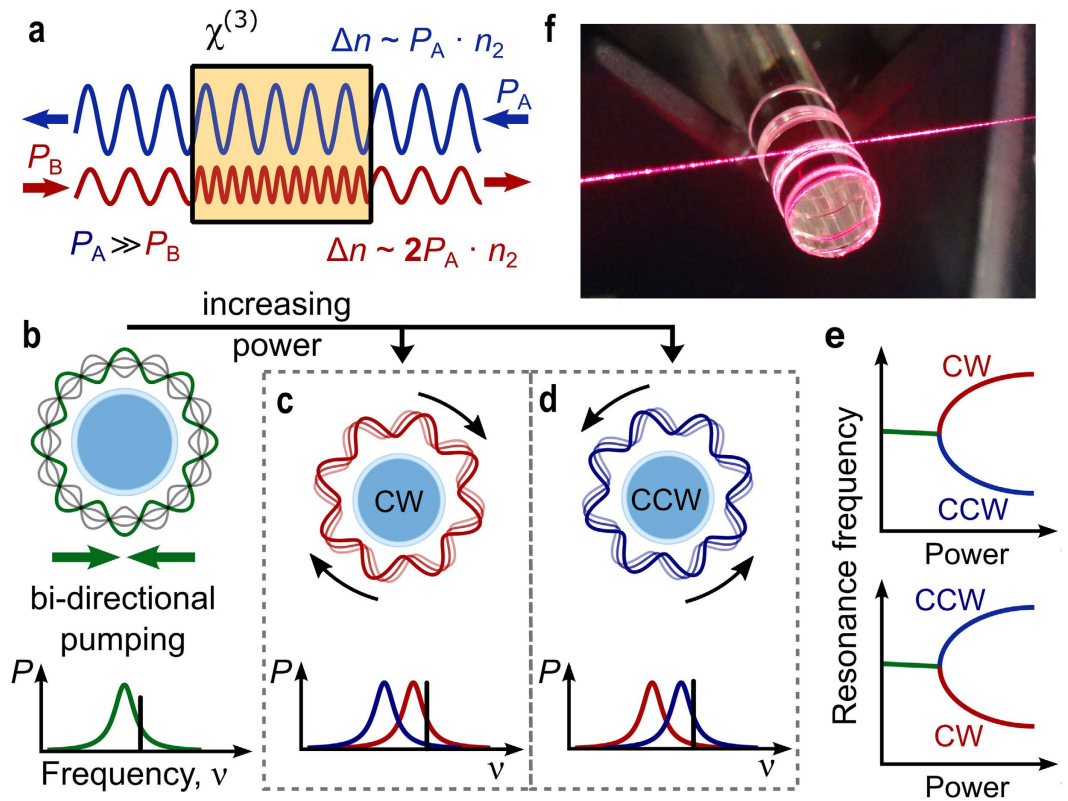


Figure 1. Nonlinear interaction between counter-propagating light. (a) Principle of Kerr-nonlinearity-mediated interaction between counter-propagating light without a resonator. Two counter-propagating but spatially overlapping light waves (offset in the diagram for clarity) with identical frequency will experience a different effective refractive index change Δn depending on their powers (P_A , P_B). The light wave with lower optical power (P_B) experiences a stronger refractive index increase, which leads to a shorter wavelength. (b) Bi-directional pumping of a whispering gallery resonator at low power, generating a standing wave. When increasing the power, the system collapses either into state (c) with clockwise propagating (CW) light or state (d) with counterclockwise (CCW) propagating light. This symmetry breaking goes along with a resonance frequency splitting between the counter-propagating optical modes (shown in the lower part of panels (b–d) where the black line denotes the pump frequency). (e) Symmetry breaking shown by the splitting between the CW and CCW resonance frequencies with increasing power. (f) Fused silica resonator and tapered fibre used in the experiments (highlighted with red laser light).

medium will have different wavelengths within the medium if their powers are unequal. This can be explained by cross-phase modulation between the two light waves, in which the weaker light wave experiences a stronger refractive index change. More specifically, the refractive index changes $\Delta n_{A,B}$ induced by the nonlinear interaction are given by

$$\Delta n_A = \frac{n_2}{A_{\text{eff}}}(P_A + 2P_B) \text{ and } \Delta n_B = \frac{n_2}{A_{\text{eff}}}(P_B + 2P_A), \quad (1)$$

with subscripts A, B indicating the two counter-propagating waves with powers $P_{A,B}$, n_2 being the nonlinear refractive index of the medium and A_{eff} being the effective mode cross-section. It is important to note that a counter-propagating light wave induces twice the refractive index change compared to the change induced by self-phase-modulation^{24,25}. In the case of an optical resonator with $\chi^{(3)}$ nonlinearity, the difference in refractive index change leads to two different optical path lengths experienced by the counter-propagating modes. This is reflected in a splitting of the resonance frequencies of the clockwise (CW) and counterclockwise (CCW) modes as shown in Fig. 1c,d. Theoretical predictions suggest that such resonators exhibit symmetry breaking when simultaneously pumped with equal power in both the CW and CCW directions^{6,7}. This may be explained by a self-amplification of small power fluctuations between the counter-propagating light. With the laser frequency at higher frequency compared to the resonance, the optical mode with infinitesimally lower power experiences a stronger Kerr-shift and is pushed further away from the pump laser frequency. Simultaneously, the stronger mode experiences less Kerr-shift and moves towards the pump laser, such that it gains even more power. This increases the resonance splitting until the system comes to a new equilibrium and self-phase modulation prevents the stronger mode from further approaching the laser (similar to thermal self-locking²⁶ of microresonator modes to a laser). For low optical powers (Fig. 1b), no splitting is induced and the CW and CCW circulating powers remain equal. Above a certain threshold power however, the state with equal coupled powers becomes unstable, and the

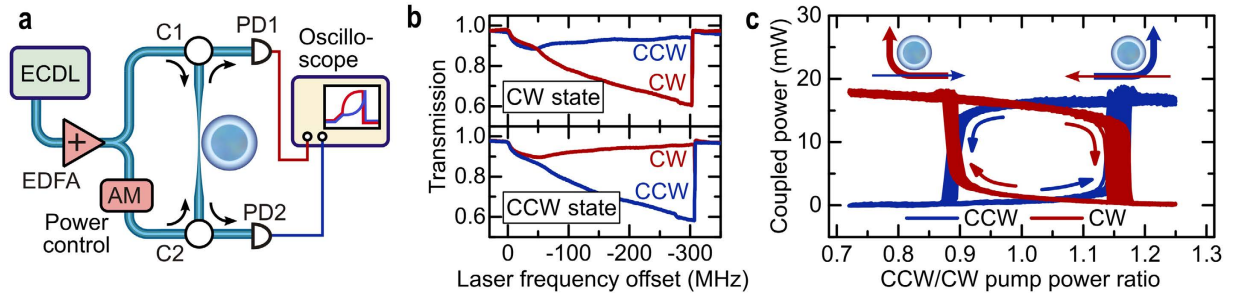


Figure 2. Experimental setup and data showing nonlinearity-induced symmetry breaking between counter-propagating light. (a) Schematic of the setup. The light of an external cavity diode laser (ECDC) is split into two parts and sent into a fused silica whispering gallery resonator from opposite directions. Two optical circulators C1, 2 split off the light coming from the microresonator and enable the measurement of the clockwise and counterclockwise transmission using photodiodes PD1 and PD2. The ratio between the counter-propagating pump powers can be adjusted using an amplitude modulator (AM). (b) Transmission vs. laser frequency measured on two consecutive laser sweeps across the resonance with equal powers of 80 mW launched in each counter-propagating direction. The system spontaneously breaks the symmetry and “picks” one of two possible states allowing light to couple in from just one direction, i.e. CW (top) or CCW (bottom). (c) Measurement of optical switching between the CW and CCW states, showing a hysteresis loop. The graph is obtained by tuning the laser into resonance and modulating the power in one direction up and down ~30 times. Inset: illustrations of the power flow in the two states.

system instead chooses one of the two states shown in Fig. 1c and d, breaking the CW-CCW symmetry. Note that the induced mode splitting should not be confused with mode splitting through backscattering of light^{27,28}. Backscattering of light in the resonator is a symmetric process such that each of the split resonances contains a superposition of the clockwise and counterclockwise propagating modes.

The optical powers that are coupled into the clockwise and counterclockwise circulating modes of a whispering gallery resonator are given by the following coupled equations (see Supplementary information for further details):

$$P_{CW} = \frac{\eta P_{in,CW}}{1 + \left(\frac{\delta}{\gamma} + \frac{1}{P_0} (P_{CW} + 2P_{CCW}) \right)^2} \quad (2)$$

$$P_{CCW} = \frac{\eta P_{in,CCW}}{1 + \left(\frac{\delta}{\gamma} + \frac{1}{P_0} (P_{CCW} + 2P_{CW}) \right)^2} \quad (3)$$

Here, $P_{in,CW}$ and $P_{in,CCW}$ are the incident pump powers, δ is the detuning of the laser frequency with respect to the resonance without Kerr shift, $\gamma = \gamma_0 + \kappa$ is the loaded half-linewidth of the resonance for intrinsic and coupling-related decay rates γ_0 and κ , and $\eta = 4\kappa\gamma_0/\gamma^2$ is the coupling efficiency. The quantity $P_0 = \pi n_0 A_{eff}/(QF_0 n_2)$ is the characteristic coupled power at which Kerr nonlinear effects occur, with n_0 and n_2 being the linear and nonlinear refractive indices for a resonator with effective cross-sectional area A_{eff} , loaded quality factor Q , and intrinsic finesse F_0 . Importantly, equations (2, 3) show that the nonlinear interaction with the counter-propagating light wave is twice as strong as the self-phase-modulation-induced interaction. This can be seen from the factor of two in the term $P_{CW} + 2P_{CCW}$ in equation (2). Moreover, an analysis of equations (2, 3) shows that for $P_{in,CW} = P_{in,CCW}$, symmetry breaking occurs when $\eta P_{in,CW}/P_0 > 8/(3\sqrt{3}) \approx 1.54$ over a range of laser detunings δ/γ that depends on the value of $\eta P_{in,CW}/P_0$. The threshold incident power for symmetry breaking is thus:

$$P_{thres.} = \frac{1.54}{\eta} \frac{\pi n_0^2 V}{n_2 \lambda Q Q_0} \quad (4)$$

where $V \approx 2\pi R A_{eff}$ is the mode volume for resonator radius R , λ is the vacuum wavelength of the laser and Q_0 is the intrinsic quality factor.

Figure 2a shows our experimental setup, which is based on a 2.7 mm diameter high-Q whispering-gallery-mode fused silica microrod resonator²⁹. The resonator has an intrinsic quality factor Q_0 of approximately 7×10^7 and an effective cross-sectional area A_{eff} of approximately $60 \mu\text{m}^2$ (see Supplementary information). Light from an amplified continuous wave external cavity diode laser (ECDC) in the $1.55 \mu\text{m}$ wavelength range is coupled into the resonator in both directions via a tapered optical fibre³⁰. A fibre-coupled electro-optic intensity modulator allows us to modulate the ratio of the pump powers $P_{in,CW}$ and $P_{in,CCW}$.

The spontaneous symmetry breaking is demonstrated in Fig. 2b. Sweeping the laser frequency across the resonance with $P_{in,CW} = P_{in,CCW}$, the coupled powers P_{CW} and P_{CCW} initially follow the same trace before abruptly diverging, randomly choosing one of two states. Note that the total resonance shift of ~300 MHz also includes a

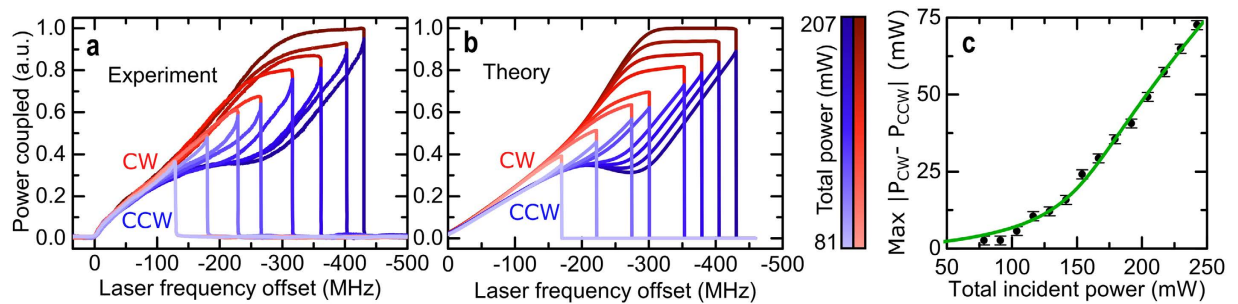


Figure 3. Threshold and power dependence of the symmetry breaking between clockwise and counterclockwise propagating light.

(a) Amount of light coupled into the resonator as a function of the laser frequency for increasing incident powers (by changing the EDFA output power, cf. Fig. 2). Higher powers (shown as darker colours) lead to an increased splitting between the clockwise (red) and counterclockwise (blue) modes. The incident power is 10% higher in the clockwise direction to avoid switching caused by fluctuations in the relative power. (b) Theoretical calculation of the power coupled into the resonator with the same parameters as in panel (a). (c) Maximum difference between clockwise and counterclockwise coupled powers as a function of the total input power. The black dots show the experimental measurements while the green curve is a theoretical fit for a pump power ratio of 0.9.

thermally induced component^{26,31} and a unidirectional Kerr shift³², which does not contribute to a resonance splitting. We observe threshold powers of ~ 10 mW, though this could be easily reduced to tens of microwatts by using chip-based resonators. In state of the art silicon nitride resonators^{33,34} the threshold power could be as low as $50 \mu\text{W}$ (assuming $Q = 1.7 \times 10^7$, $n_2 = 2.4 \times 10^{-15} \text{ cm}^2/\text{W}$, diameter = $50 \mu\text{m}$, $A_{\text{eff}} = 1 \mu\text{m}^2$). An interesting feature of the nonlinearity induced symmetry breaking is hysteresis, which is shown in Fig. 2c. Holding the laser frequency constant within the bistable regime, we modulate $P_{\text{in,CCW}}$ at 5 kHz by $\pm 25\%$. The observed hysteresis can be explained by the resonance frequency splitting in the two stable states. To overcome the resonance splitting and switch into the other state, the initially weaker pump direction has to be significantly increased to a power well above that of the counter-propagating pump light. Notably, this hysteresis allows the system to be used as an all-optical flip-flop or binary memory unit^{20,21}. Since this process is mediated by the almost instantaneous Kerr effect, the switching times are only limited by the cavity lifetime. In the presented data this is on the order of 30 ns, however this could be significantly reduced in a material with lower Q-factor and higher nonlinearity (e.g. < 1 ns in a silicon nitride resonator with $Q = 3 \times 10^6$, diameter = $50 \mu\text{m}$, $A_{\text{eff}} = 1 \mu\text{m}^2$ at 2 mW optical power). Moreover, the non-reciprocal light propagation in each of the stable states can be exploited to realise optically switchable circulators or isolators (cf. Fig. 2b).

The amplification of power imbalances is tested against the theory in Fig. 3a and b. Here the laser frequency is scanned across the resonance for a range of total pump powers, while keeping the ratio $P_{\text{in,CCW}}/P_{\text{in,CW}}$ fixed at 0.9. At low pump powers, no resonance frequency splitting is observed and the two counter-propagating modes show the same profiles when sweeping across the resonance (lowest power curve in Fig. 3a). Increasing the power, the effect of the cross-phase modulation induced Kerr shift leads to a large difference between the coupled powers. The theoretical results shown in Fig. 3b use the same parameters as employed experimentally in Fig. 3a. Included in the calculations is a thermally induced frequency shift^{26,31}. A fit of the maximum coupled power difference vs. total pump power (Fig. 3c) is in excellent agreement with the measured data. Small deviations between the curves in Fig. 3a and b may be attributed to modelling the system using the assumption that the thermal shift of the resonance frequency is immediate, whereas in reality it has a delayed response³¹.

Figure 4 shows additional comparisons between our experimental results and theoretical simulations of the symmetry breaking between counterpropagating light in resonators. Figure 4a includes colour-coded solutions for launching unequal powers into a microresonator.

In conclusion, we demonstrate the observation of spontaneous symmetry breaking between counter-propagating light in a nonlinear resonator by pumping an optical microresonator equally in the clockwise and counterclockwise directions. Our results closely match our theoretical predictions based on nonlinear interaction between counter-propagating light induced by the Kerr nonlinearity. We show that above a threshold power, a symmetry-broken regime exists as first predicted by Kaplan and Meystre^{6,7}. Several potentially far-reaching applications are proposed for this effect. The observed symmetry breaking represents arguably the most fundamental way to induce optical non-reciprocity, which is urgently needed for chip-integrable optical diodes and circulators for forthcoming waveguide coupled lasers. Moreover, the observed hysteresis will allow the realisation of all-optical flip-flops^{20,21} for photonic memories and data processing. Calculations show that smaller resonators with higher nonlinearity (e.g. state of the art silicon nitride resonators³⁴) enable threshold powers of a few tens of microwatts and switching speeds exceeding 1 GHz at power levels of a few milliwatts. In addition, just below the threshold of the symmetry breaking, the state of the system is exceptionally sensitive to minute imbalances between the clockwise and counter-clockwise circulating light⁶. This enables a range of enhanced sensors for optical power, refractive index⁹ and rotation^{6,8}, as well as new types

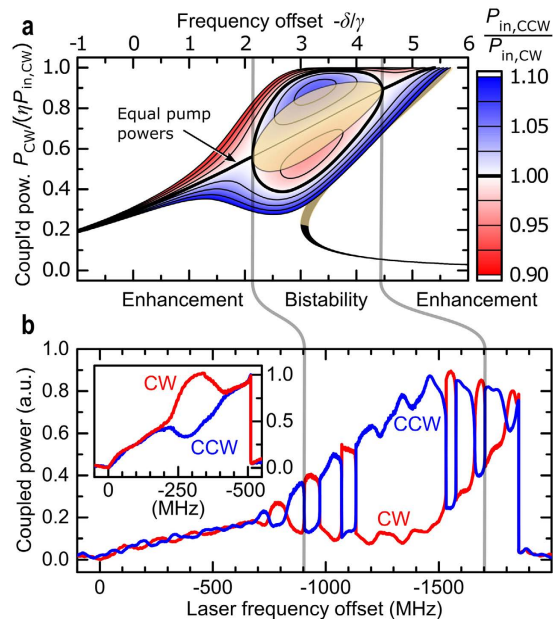


Figure 4. Different regimes of nonlinearity-induced mode splitting. (a) Theoretical prediction for the power P_{CW} coupled into the resonator in the clockwise direction as a function of the normalised laser detuning frequency δ/γ . The incident power imbalance is colour-coded with red (blue) contours corresponding to higher power in the CW (CCW) direction. The bold black curve shows spontaneous symmetry breaking in the case of equal pump powers. In this region between the two grey lines, two stable solutions exist for a range of power imbalances. The beige shaded area contains unstable solutions. (b) Scan of the laser frequency across the resonance while backscattering-induced interference effects in the setup cause $P_{in,CCW}/P_{in,CW}$ to change about unity by $\pm 3\%$ at a period of ~ 170 MHz in the laser frequency. The launched power is 180 mW in each direction. Outside the grey lines the coupled power difference is enhanced with respect to the incident power imbalance by the non-reciprocal Kerr shift. The enhancement increases approaching the bistable regime, in which the system begins to jump between the two stable configurations. The inset shows a sweep across a microresonator mode with equal power and no interference effects, leading to a “bubble”-shaped symmetry-broken region corresponding to the bold black trace in panel (a).

of near-field probes. Besides these immediate practical applications, the symmetry breaking shows significant potential for a variety of novel concepts in basic research and for future advanced integrated photonic circuits. Most importantly, the fundamental nature of symmetry breaking in resonant states with periodic boundary conditions through nonlinear coupling could impact science beyond optical physics e.g. in acoustic waves, quantum mechanical wave functions, and microwave resonators.

Note added: we would like to draw the reader’s attention to a related recent work³⁵.

References

- Ezekiel, S., Hellwarth, R. W. & Davis, J. L. Observation of intensity-induced nonreciprocity in a fiber-optic gyroscope. *Opt. Lett.* **7**, 457–459 (1982).
- Menon, V., Tong, W., Xia, F., Li, C. & Forrest, S. Nonreciprocity of counterpropagating signals in a monolithically integrated Sagnac interferometer. *Optics Letters* **29**, 513–515 (2004).
- Gelens, L. *et al.* Exploring multistability in semiconductor ring lasers: Theory and experiment. *Physical review letters* **102**, 193904 (2009).
- Trita, A. *et al.* All-Optical Directional Switching in Bistable Semiconductor-Ring Lasers. *IEEE Journal of Quantum Electronics* **49**, 877–885 (2013).
- Trita, A. *et al.* 10 Gb/s Operation of Monolithic All-Optical Set-Reset Flip-Flop Based on Semiconductor Ring Laser. *Conference on Lasers and Electro-Optics 2010 CThN3*, doi: 10.1364/CLEO.2010.CThN3 (2010).
- Kaplan, A. E. & Meystre, P. Enhancement of the Sagnac effect due to nonlinearly induced nonreciprocity. *Optics Letters* **6**, 590–2 (1981).
- Kaplan, A. E. & Meystre, P. Directionally asymmetrical bistability in a symmetrically pumped nonlinear ring interferometer. *Optics Communications* **40**, 229–32 (1982).
- Wang, C. & Search, C. P. Enhanced rotation sensing by nonlinear interactions in silicon microresonators. *Optics Letters* **39**, 4376–4379 (2014).
- Wang, C. & Search, C. P. A Nonlinear Microresonator Refractive Index Sensor. *Journal of Lightwave Technology* **33**, 4360–4366 (2015).
- Potton, R. J. Reciprocity in optics. *Reports On Progress In Physics* **67**, PII S0034–4885(04)26328–X (2004).
- Feng, L. *et al.* Nonreciprocal Light Propagation in a Silicon Photonic Circuit. *Science* **333**, 729–733 (2011).
- Peng, B. *et al.* Chiral modes and directional lasing at exceptional points. *Proceedings of the National Academy of Sciences* **113**, 6845–6850 (2016).
- Peng, B. *et al.* Parity-time-symmetric whispering-gallery microcavities. *Nature Physics* **10**, 394–8 (2014).
- Chang, L. *et al.* Parity-time symmetry and variable optical isolation in active-passive-coupled microresonators. *Nat Photon* **8**, 524–529 (2014).
- Fan, L. *et al.* An all-silicon passive optical diode. *Science* **335**, 447–450 (2012).
- Haldane, F. D. M. & Raghu, S. Possible realization of directional optical waveguides in photonic crystals with broken time-reversal symmetry. *Physical Review Letters* **100**, 013904 (2008).

17. Kono, N., Kakihara, K., Saitoh, K. & Koshiba, M. Nonreciprocal microresonators for the miniaturization of optical waveguide isolators. *Optics express* **15**, 7737–7751 (2007).
18. Shu, F.-J., Zou, C.-L., Zou, X.-B. & Yang, L. Chiral Symmetry Breaking in Micro-Ring Optical Cavity By Engineered Dissipation. *arXiv preprint arXiv:1604.08678* (2016).
19. Yu, Z. & Fan, S. Complete optical isolation created by indirect interband photonic transitions. *Nature Photonics* **3**, 91–94 (2009).
20. Daniel, B. A. & Agrawal, G. P. Phase-Switched All-Optical Flip-Flops Using Two-Input Bistable Resonators. *Ieee Photonics Technology Letters* **24**, 479–481 (2012).
21. Haelterman, M. All-optical set-reset flip-flop operation in the nonlinear Fabry-Perot interferometer. *Optics Communications* **86**, 189–91 (1991).
22. Liu, L. *et al.* An ultra-small, low-power, all-optical flip-flop memory on a silicon chip. *Nature Photonics* **4**, 182–187 (2010).
23. Soljacic, M. *et al.* Switching through symmetry breaking in coupled nonlinear micro-cavities. *Optics express* **14**, 10678–10683 (2006).
24. Chiao, R. Y., Kelley, P. L. & Garmire, E. Stimulated four-photon interaction and its influence on stimulated rayleigh-wing scattering. *Physical Review Letters* **17**, 1158–1161 (1966).
25. Kaplan, A. E. Light-induced nonreciprocity, field invariants, and nonlinear eigenpolarizations. *Optics Letters* **8**, 560–2 (1983).
26. Carmon, T., Yang, L. & Vahala, K. J. Dynamical thermal behavior and thermal self-stability of microcavities. *Optics Express* **12**, 4742–4750 (2004).
27. Kippenberg, T. J., Spillane, S. M. & Vahala, K. J. Modal coupling in traveling-wave resonators. *Optics Letters* **27**, 1669–1671 (2002).
28. Weiss, D. S. *et al.* Splitting of high-Q Mie modes induced by light backscattering in silica microspheres. *Opt. Lett.* **20**, 1835–1837 (1995).
29. Del'Haye, P., Diddams, S. A. & Papp, S. B. Laser-machined ultra-high-Q microrod resonators for nonlinear optics. *Applied Physics Letters* **102**, 221119 (2013).
30. Knight, J. C., Cheung, G., Jacques, F. & Birks, T. A. Phase-matched excitation of whispering-gallery-mode resonances by a fiber taper. *Optics Letters* **22**, 1129–1131 (1997).
31. Ilchenko, V. S. & Gorodetsky, M. L. Thermal Nonlinear Effects in Optical Whispering Gallery Microresonators. *Laser Physics* **2**, 1004–1009 (1992).
32. Treussart, F. *et al.* Evidence for intrinsic Kerr bistability of high-Q microsphere resonators in superfluid helium. *The European Physical Journal D - Atomic, Molecular, Optical and Plasma Physics* **1**, 235–238 (1998).
33. Ikeda, K., Saperstein, R. E., Alic, N. & Fainman, Y. Thermal and Kerr nonlinear properties of plasma-deposited silicon nitride/silicon dioxide waveguides. *Optics express* **16**, 12987–12994 (2008).
34. Xuan, Y. *et al.* Ultra-high-Q Silicon Nitride Micro-Resonators for Low-Power Frequency Comb Initiation. *Conference on Lasers and Electro-Optics JW2A.75* (2016).
35. Cao, Q.-T. *et al.* Experimental demonstration of spontaneous chirality in a nonlinear microresonator. *Physical Review Letters* **118**, 033901 (2017).

Acknowledgements

This work has been supported by the National Physical Laboratory Strategic Research Programme. LDB is supported by the Engineering and Physical Sciences Research Council (EPSRC) through the Centre for Doctoral Training in Applied Photonics.

Author Contributions

P.D., L.D.B. and J.M.S. conceived the experiments. J.M.S., L.D.B. and S.L.S. designed and performed the experiments. All authors contributed to the manuscript.

Additional Information

Supplementary information accompanies this paper at <http://www.nature.com/srep>

Competing financial interests: The authors declare no competing financial interests.

How to cite this article: Del Bino, L. *et al.* Symmetry Breaking of Counter-Propagating Light in a Nonlinear Resonator. *Sci. Rep.* **7**, 43142; doi: 10.1038/srep43142 (2017).

Publisher's note: Springer Nature remains neutral with regard to jurisdictional claims in published maps and institutional affiliations.



This work is licensed under a Creative Commons Attribution 4.0 International License. The images or other third party material in this article are included in the article's Creative Commons license, unless indicated otherwise in the credit line; if the material is not included under the Creative Commons license, users will need to obtain permission from the license holder to reproduce the material. To view a copy of this license, visit <http://creativecommons.org/licenses/by/4.0/>

© The Author(s) 2017